

3-D Numerical Analysis of a Carburetor Performance for different Air-Fuel Ratios

Hanoca P¹, Murganandan S²

¹Assistant Professor, Department of Mechanical Engineering, Rajeev Institute of Technology, Hassan, Karnataka, India.

²Automation Engineer, Indo-MIM Pvt. Ltd., Hoskote, Karnataka, India-562114.

Abstract - Due to price constraints, small engines rely on inexpensive and mechanically simple devices for air fuel mixture formation in carburetors. A typical carburetor consists of a complex set of internal passages designed to deliver the engine the correct air fuel mixture according to speed and load. This project comprises the Computational Fluid Dynamics (CFD) analysis to investigate the flow behavior of three dimensional venturi of a carburetor. Steady state analysis were carried out at different air fuel ratio and different mass flow rates to obtain the overall performance using commercial CFD software ANSYS FLUENT. We have carried out the analysis for different values of air fuel ratio varying from 14.5:1, 16.5:1, 18.5:1 and mass flow rate varying from 0.0004kg/s, 0.0005kg/s and 0.0006kg/s. Also for two different cases namely only with carburetor venturi, carburetor venturi with nozzle. For all the above mentioned variations we have obtained pressure, velocity and turbulence kinetic energy contours and their respective graphs.

Key Words: CFD of carburetor, Venturi analysis, Air fuel mixture in engines.

ABBREVIATIONS

IC	: Internal Combustion
SI	: Spark Ignition
CI	: Compression Ignition
CFD	: Computational Fluid Dynamics
FEA	: Finite Element Analysis
CAD	: Computer Aided Drawing
FDM	: Finite Difference Method
FVM	: Finite Volume Method
BEM	: Boundary Element Method
FEM	: Finite Element Method
V-N	: Venturi with Nozzle

V-N-B : Venturi with nozzle and Baffle plate

MFR : Mass Flow Rate

NOMENCLATURE

m/s : Meter per Second

Pa : Pascal

Kg/s : Kilogram per second

m²/s² : Meter square per second square

m : Meter

1. INTRODUCTION

Internal combustion engines are seen every day in automobiles, trucks, and Buses. The name internal combustion refers also to gas turbines except that the name is usually applied to reciprocating internal combustion (I.C.) engines like the ones found in everyday automobiles. There are basically two types of I.C. ignition engines, those which need a spark plug, and those that rely on compression of a fluid. Spark ignition engines take a mixture of fuel and air, compress it, and ignite it using a spark plug. The process of forming a combustible fuel air mixture by mixing the right amount of fuel with air before admission to the cylinder of the engine is called carburetion and the device is known as a carburetor.

Several experimental and numerical investigations have been performed in the past. Prof. Laxmikant P. Narkhede, Prof. V.H. Patil and Prof. Atul Patil [1] performed 2D CFD Simulations of nozzle flow analysis for Carburetor to increase the volumetric efficiency of engine and to check the mass flow rate of air on a bend L-shape venturi nozzle pipe. Results shows the flow pattern at the outlet of the carburetor with plot showing the contours for gas mass fraction, for a total mass flow rate of 0.026kg/s i.e. 94kg/hr. and analytical calculation shows the result mass flow rate of 0.0273kg/s (98kg/hr.).

Shashwat Sharma, Prateek Jain and Adhar Singh [2] had studied on optimization of Flow through Venturi of Carburetor. The analysis was done for $\theta = 30^\circ, 35^\circ, 40^\circ, 45^\circ$ where θ is the angle between the axis of the fuel

discharge nozzle and the vertical axis of the body of the carburetor. And finally concluded that when analysed for fuel discharge nozzle angle of 30° which leads to better optimization and vaporization of the fuel inside the carburetor with uniform pressure distribution but in other cases a fuel discharge nozzle angle at 35° or 40° the pressure distribution is quite non uniform inside the body of the carburetor. So that for gasoline operated engine the optimum fuel discharge nozzle angle is 30° . Rangu P, Ganesha T, M.C. Math[3] has reviewed the work on CFD analysis of a simple carburetor to find pressure drop and velocity profile for different throttle angle($30, 40, 50, 60, 70, 80$ and 90) and fuel discharge nozzle angle($33, 36, 39$). The result obtained from the analysis are analysed for optimum design of a carburetor in which maximum pressure were observed at the throttle angle of 90° . The pressure distribution was observed more uniform at the fuel discharge nozzle angle of 33° .

J Suresh Kumar, V Ganesan, J M Mallikarjuna and S Govindarajan [4] studied on design and optimization of a throttle body assemble for single cylinder engine used in two wheeler application has been analysed with investigation of critical flow through various subsystem using CFD and results were observed that the air flow through main and bypass passage are almost same around 12% throttle opening and air flow through main passage takes over beyond 25% opening. Also every 2mm increased in throttle valve diameter, the increased in air flow is about 7% at wide open throttle conditions and at part throttles openings. The increase in air flow is by about 6%. Terry L. Hendricks [5] carried out a numerical and experimental fuel flow analysis of small engine carburetor. He concluded that the pressure loss across the idle discharge metering orifice, which effectively simulates expansion into the engine manifold.

Reviewing the above paper, it is clearly noticed that commercial 3D Computational Flow Dynamics (CFD) code ANSYS FLUENT to study the different air-fuel ratio for velocity of air at $8.267\text{m/s}, 10.336\text{m/s}$ and 12.404m/s . The second aim was to study the *contours of static pressure, gauge total pressure, velocity magnitude and turbulence kinetic energy inside the Venturi of carburetor.*

2. METHODOLOGY

The schematic of the model is shown in the Fig-1.



Fig-1: Simple carburetor model.

Specification of the model

1. Total length of carburetor	= 59mm
2. Inlet Diameter	= 27mm
3. Throat Diameter	= 17mm
4. Outlet Diameter	= 21mm
5. Length of Throat	= 4mm
6. Length of inlet Part	= 23mm
7. Length of Outlet Part	= 32mm
8. Nozzle Diameter	= 3mm

2.1 CFD ANALYSIS OF FLOW DOMAIN

2.1.1 Modeling

The flow domain of the Carburetor Venturi was created by Solid Edge software as in Fig-2. The model was considered for flow analysis to reduce grid size thereby reducing computation time. 3 dimensional modeling flow domain of the Carburetor Venturi and Carburetor venturi with nozzle and baffle plate is shown in Fig-3.1 and Fig-3.2.



Fig-2: 2D sketch of flow domain according to dimensions.

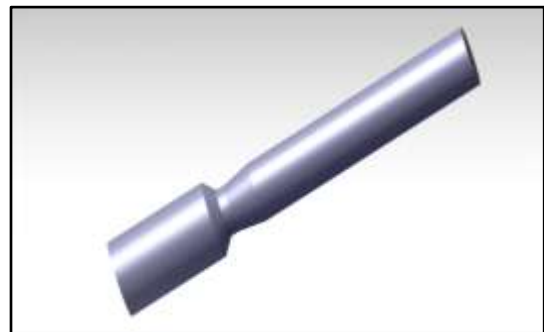


Fig-3.1: 3D modeling of flow domain Venturi.

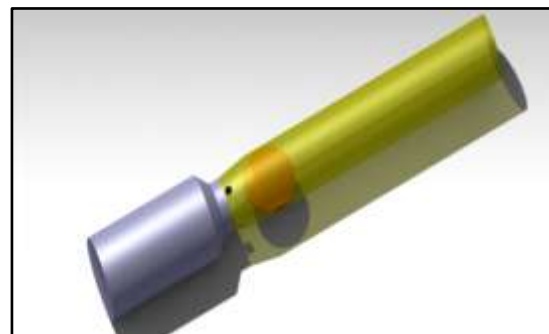


Fig-3.2: 3D modeling of flow domain with Venturi with Nozzle and baffle plate.

2.1.2 Meshing

Meshing was done in ANSYS ICEM CFD. 3D solid model of Carburetor Venturi in 'step' format was imported to ICEM CFD. As per the requirements of the model blocking and structural meshing was done. Lot of effort has been taken to make a structural mesh for a complete flow domain to conduct the numerical analysis. Very fine mesh was created around the surface of Nozzle inlet and Venturi in order to capture near wall or boundary layer flow over it. Structured grid takes less computation time and memory usage. CFD solvers converge better and generate more precise results when the grid is associated with the predominant flow direction. Structured mesh of solid flow domain with Venturi is shown in Fig-4. Structured mesh with Venturi and Nozzle is shown in Fig-5. It can be observed that extremely fine mesh is generated to capture the flow behavior over the carburetor.

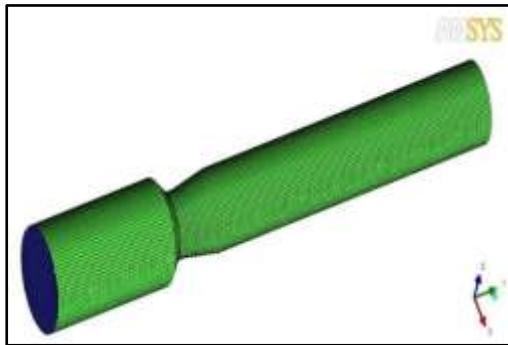


Fig-4: Structured meshing of flow domain with Carburetor venturi only.



Fig-5: Layer section of structured meshing Venturi with Nozzle and baffle plate.

2.1.3 Flow Analysis

3-D steady Navier-Stoke equations were solved using segregated pressure based implicit solver by ANSYS FLUENT. Realizable Steady air flow across carburetor Venturi with nozzle and Baffle Plate (a) Static pressure [Pa] (b) Gauge total pressure [Pa] (c) Turbulent kinetic energy [m²/s²] (d) Velocity magnitude [m/s] was used for the analysis.

2.1.4 Boundary Conditions

Wall boundary conditions were specified for Baffle Plate and Nozzle wall. Velocity inlet condition was specified for the inlet of the Air Inlet and Fuel Inlet. Outlet condition was allotted for the Outlet Flow of the Air-Fuel mixture. Interior condition was allotted for the Inlet Fluid. The specified boundary conditions are shown in Table-1 and Fig-6.

Table -1: Boundary conditions

Boundary condition	Boundary surface
Wall	Baffle Plate
Wall	Nozzle Wall
Velocity inlet	Inlet
Velocity inlet	Fuel Inlet
Interior	Inlet Fluid
Outlet	Outlet Flow

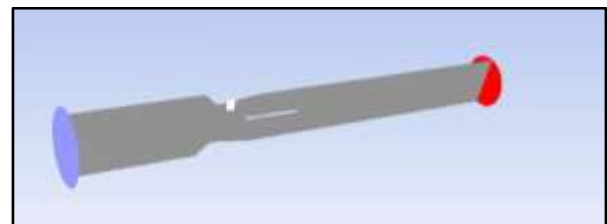


Fig-6: Boundary Condition for venturi of the carburetor.

2.1.5 Solution methodology

The meshed domain was computed in FLUENT until the solution was converged. The residuals were set to stop the solution once they dropped below a certain value. Figure shows the convergence history of wall Y⁺ value.

2.1.6 Grid independence test

In order to make sure that the solution is not affected by the amount of the grid, a grid independence study was carried out for different cell sizes and wall Y⁺ value was determined for each case. The wall Y⁺ is a non-dimensional distance similar to local Reynolds number, often used in CFD to describe how coarse or fine a mesh is for a particular flow.

- In case 1, a fine mesh was created with 116960 cells and the obtained wall Y⁺ value for a mass flow rate of 0.0004kg/s, 0.0005kg/s and 0.0006kg/s are 14.159, 17.031 and 19.884 respectively.
- In case 2, a fine mesh was created with 247160 cells and the obtained wall Y⁺ value for consequent mass flow rate and value are obtained.

By observing above cases, the value of case1 and case 2, case 1 is selected for further analysis in order to reduce the computation time. Table-2 shows the wall Y+ values for different mass flow rate for two different cases. Figure shows the plot of wall Y+ values for all the two cases.

Table-2: Grid independence test

Case	Cell size	Y+ for 0.0004 kg/s	Y+ for 0.0005 kg/s	Wall Y+ for 0.0006 m/s
1	116960	14.159	17.031	19.884
2	247160	11.292	13.406	15.553

3. RESULTS AND DISCUSSION

CFD analysis was carried out for different Air-Fuel Ratio of 14.5:1, 16.5:1, 18.5:1 and mass flow rate varying from 0.0004kg/s, 0.0005kg/s and 0.0006kg/s as shown in the table 3 using ANSYS FLUENT.

The following results will be explained.

Table-3: Different mass flow rate

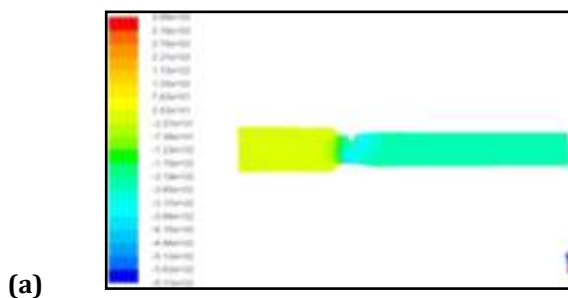
MFR Kg/s	Velocity of Fuel m/s	Velocity of Air m/s
0.0004	0.0785	8.269
0.0005	0.0982	10.366
0.0006	0.1178	12.404

3.1 Contours of Flow across

3.1.1 Carburetor Venturi with Nozzle

The presence of the fuel tube resulted in a strong change in the flow field in the carburetor venturi. Fig-7, Fig-8 and Fig-9 shows the effect of a nozzle with diameter equal to 3 mm. The presence of the fuel tube produced a reduced cross-sectional throat area and a large wake zone behind it. This wake changes completely the nature of the pressure losses and effective area for the flow downstream of the venturi throat.

3.1.1[A] For Mass Flow Rate of 0.0004 kg/s



(b)

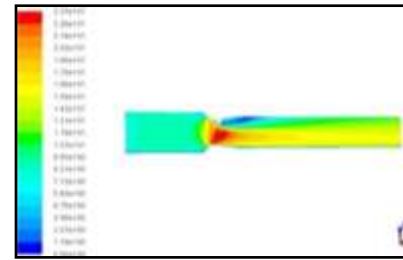
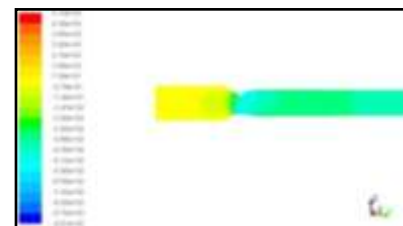


Fig-7: Steady air flow across carburetor venturi with nozzle (a) Static pressure [Pa] (d) Velocity magnitude [m/s]

3.1.1[B] For Mass Flow Rate of 0.0005 kg/s

(a)



(b)

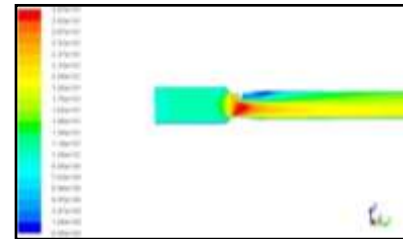
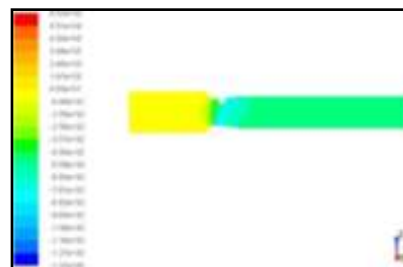


Fig-8: Steady air flow across carburetor venturi with nozzle (a) Static pressure [Pa] (d) Velocity magnitude [m/s]

3.1.1[C] For Mass Flow Rate of 0.0006 kg/s

(a)



(b)

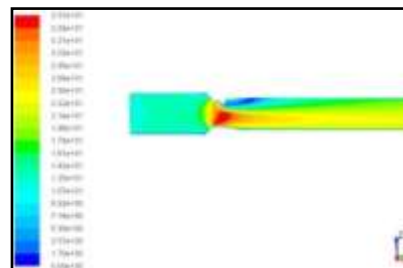


Fig-9: Steady air flow across carburetor venturi with nozzle (a) Static pressure [Pa] (d) Velocity magnitude [m/s]

The static pressure is almost constant in the radial direction, with the exception at the venturi throat, where the static pressure changes next to the wall. Constant pressure in the cross-section everywhere but in the venturi throat at this location there is a different static pressure in the radial direction. In addition, the sharp leading edge of the fuel tube creates a separation region, which results in a lower pressure at the tip of the fuel tube downstream of the fuel tube, the static pressure is almost constant in the radial and axial directions.

The velocity field shows the wake region created by the fuel tube. The final effect of the fuel tube on the airflow is to reduce the effective area used by the flow behind the venturi. The size of the wake region is increased with the size of the fuel tube. This wake zone may be responsible for fuel puddling after the carburetor: once a fuel droplet is captured in this region, there is no momentum to drive it downstream of the carburetor. As the analysis was performed with the same pressure difference for all of the venturi geometries, the effect of the fuel tube is a reduced mass flow rate of air. If the analysis were performed at constant flow rate, the mass conservation in the reduced area would have produced a higher velocity and lower static pressure. These images allow for a better understanding of the complex interaction between the fuel tube and the air flow in the current carburetor designs, a fuel tube extending into the venturi throat, beyond the throat wall, is necessary. It brings the fuel flow near the centerline of the venturi, which is intended to help generate an even distribution of the droplets in the flow field. A fuel tube that does not extend beyond the wall would not prevent the fuel flow from staying next to the wall. But the fuel tube itself also completely disturbs the airflow, increasing the pressure losses and, therefore, decreasing the mass flow rate at a given pressure drops.

3.1.2 Carburetor Venturi with Nozzle and Baffle Plate

Besides the intake valves, the throttle plate is the largest restriction to the air flow in the intake manifold. The carburetor venturi was simulated with the inlet obstacles, fuel tube and throttle plate. The throttle plate was modelled as similarly as possible to the physical model; it was composed of the axis rod, the plate and the screw. Fig-10, Fig-11 and Fig-12 shows that the throttle plate angle causes a large effect on the flow field, increasing the wake zone and also producing asymmetric features in the flow. The static pressure field does not change significantly from the previous cases; additional stagnation points are created by the leading edge of the throttle plate, shaft and screw. However, the velocity field is greatly influenced by the throttle plate: the high speed stream created by the fuel tube now encounters a large obstacle just downstream. The wakes created by the fuel

tube and the throttle plate, axis and screw interact between them, producing a vortex shedding seen in both planes. These wake regions increase the potential for fuel puddling. In addition, the flow field shows that, even at wide open conditions, the screw creates an asymmetry in the flow. The highest velocity on the right side of the throttle plate (seen on the top view) shows that that side of the flow would get a higher air flow, and, it may be inferred, more fuel droplets. The turbulent kinetic energy indicates that the throttle plate, shaft and screw are responsible for the largest turbulence in the flow. This turbulence produces a reduced isentropic stagnation pressure.

3.1.2[A] For Mass Flow Rate of 0.0004 kg/s

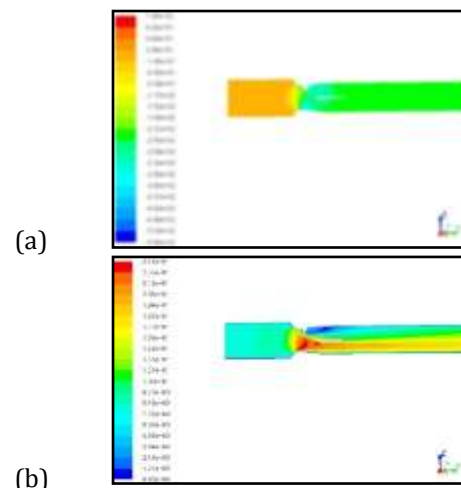


Fig-10: Steady air flow across carburetor venturi with nozzle (a) Static pressure [Pa] (b) Velocity magnitude [m/s]

3.1.2[B] For Mass Flow Rate of 0.0005 kg/s

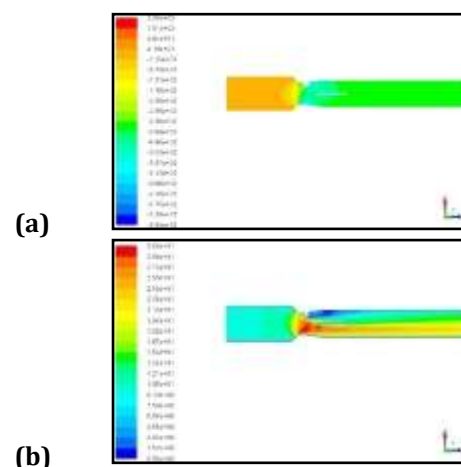


Fig-11: Steady air flow across carburetor venturi with nozzle (a) Static pressure [Pa] (b) Velocity magnitude [m/s]

3.1.2[C] For Mass Flow Rate of 0.0006 kg/s

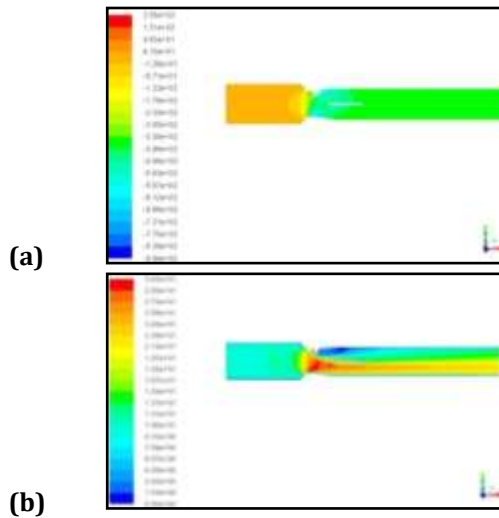


Fig-12: Steady air flow across carburetor venturi with nozzle (a) Static pressure [Pa] (d) Velocity magnitude [m/s]

3.2 Graphs and Plots for Air Fuel Ratio of 14.5:1

3.2.1 Axis of the Carburetor V/S Velocity of the Air

The Fig-13 shows the graph for axis of carburetor v/s velocity of air for mass flow rate of 0.0004 kg/s, 0.0005kg/s and 0.0006kg/s respectively. The position of the baffle plate is 90° with respect to the axis of the carburetor.

1. The behavior of velocity of air along the centerline of the venturi for different mass flow rate is shown in Fig.13.
2. The velocity of the air increases along the axis of the carburetor and reaches highest at the venturi throat.
3. In carburetor venturi and carburetor venturi with nozzle, after the mixture is passed the venturi throat the velocity of air will decreased slightly and become constant at the outlet.
4. In carburetor venturi with nozzle and baffle plate, the velocity of air decreased considerably due to the presence of baffle plate.
5. After the mixture passes the baffle plate, the velocity of air increased slightly and become constant at the outlet.

3.2.2 Axis of the Carburetor V/S Velocity of the Fuel

The Fig-14 shows the graph for axis of carburetor v/s velocity of fuel for mass flow rate of 0.0004 kg/s, 0.0005kg/s and 0.0006kg/s respectively. The position of

the baffle plate is 90° with respect to the axis of the carburetor.

1. The behavior of velocity of fuel along the centre line of the venturi for different mass flow rate is shown in Fig. 14.
2. Since the fuel enters at the throat, initially the velocity of fuel will be zero.
3. In carburetor venturi with nozzle, the velocity of fuel increased up to a certain level and then it is decreased slightly and becomes constant at the outlet.
4. In carburetor venturi with nozzle and baffle plate, the velocity of fuel increased up to a certain level due to suction of the fuel and decreased considerably due to the presence of baffle plate along the flow domain and becomes constant at the outlet.

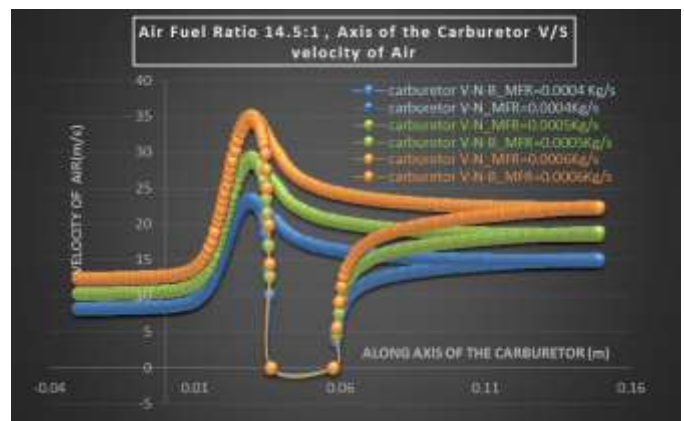


Fig-13: Axis of the Carburetor V/S Velocity of Air graph

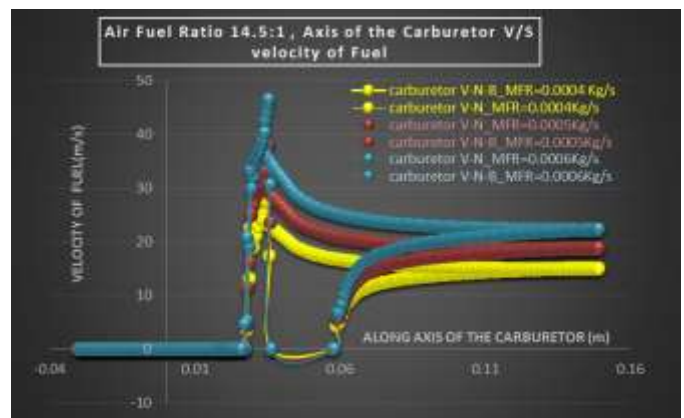


Fig-14: Axis of the Carburetor V/S Velocity of the Fuel graph

3.2.3 Axis of the Carburetor V/S Static Pressure

The Fig-15 shows the graph for axis of carburetor v/s static pressure for mass flow rate of 0.0004 kg/s, 0.0005kg/s and 0.0006kg/s respectively. The position of

the baffle plate is 90° with respect to the axis of the carburetor.

1. The behavior of static pressure along the centerline of the venturi for different mass flow rate is shown in Fig. 15.
2. The static pressure is almost constant at the inlet and outlet of the venturi, showing a slight decrease at the outlet due to frictional losses in the straight pipe section.
3. The static pressure is lowest at the venturi throat and it is increased after the air fuel mixture passed venturi throat.
4. In all of the cases the pressure decreases at the inlet of the converging section and reaches a minimum at the throat.
5. In case of carburetor venturi with nozzle and baffle plate there is a sudden increase and decrease in the static pressure due to the presence of baffle plate and at the outlet the pressure tends to be in constant.

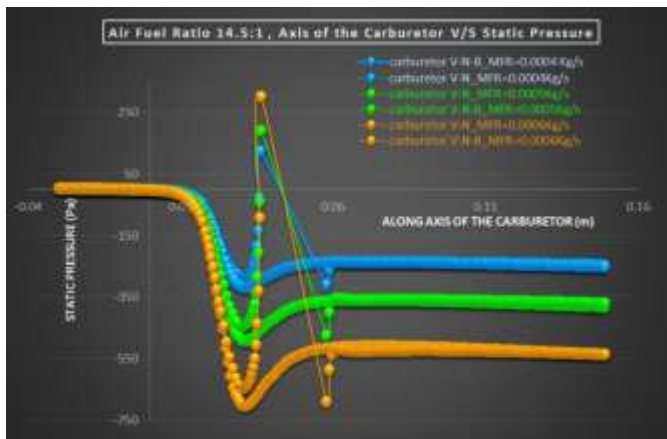


Fig-15: Axis of the Carburetor V/S Static Pressure graph

4. CONCLUSIONS

Present study shows how the result varies by changing air fuel mixture and mass flow rates inside the venturi of a carburetor. The variations through the venturi of a carburetor along with nozzle and baffle plate were determined and plotted.

We have carried out the analysis by varying the air fuel ratios like 14.5:1, 16.5:1 and 18.5:1. Pressure, velocity and turbulence kinetic energy contours and graphs were determined, studied and plotted respectively. Also we have carried out the analysis for different mass flow rates like 0.0004kg/s, 0.0005kg/s and 0.0006kg/s. Pressure, velocity and turbulence kinetic energy contours and graphs were determined, studied and plotted respectively.

Variation in pressure and velocity for cases like only venturi, venturi with nozzle and venturi with nozzle and baffle plate are studied.

REFERENCES

- [1] Shivkumar, Biradar, Ebinezar, Raj Reddy, Validation of producer gas carburetor using CFD. International Journal of Latest Research in Science and Technology, pp.90-94, 2013.
- [2] Shashwat and all, Optimization of Flow through Venturi of a Carburetor, International Journal of Scientific Engineering and Technology, pp. 570-573, 2013.
- [3] Ganeshan V, Internal Combustion Engines, Edition 2 New Delhi TMH, 2009.
- [4] Sayma Abdulnaser, Computational Fluid Dynamics, ISBN- 978-87-7681-938-4, Abdul Naser Sayma and Ventus Publishers, 2009.
- [5] Diego A. Arias, Timothy, A. Shedd, Numerical and experimental study of air and fuel flow in small engine carburetors, University of Wisconsin Madison, 2005.
- [6] Praxair, Inc. Material Safety Data Sheets for Propane, CNG, and Hydrogen, Danbury, CT USA. September 2004.
- [7] American Petroleum Institute (API), Alcohols and Ethers, Publication No. 4261, 3rd ed., June 2001.
- [8] C. Borusbay and T. Nejat Veziroglu, "Hydrogen as a Fuel for Spark Ignition Engines," Alternative Energy Sources VIII, Research and Development, Volume II, pp. 559-560, 1989.
- [9] API Technical Data Book – Petroleum Refining, Volume I, Chapter I. Revised Chapter 1 to First, Second, Third and Fourth Editions, 1988.
- [10] Petroleum Product Surveys, Motor Gasoline, National Institute for Petroleum and Energy Research, 1986.
- [11] Handbook of Chemistry and Physics, the Chemical Rubber Company Press, Inc., 62nd Edition, 1981.

BIOGRAPHIES



Mr. Murganandan S

Obtained B.E Degree in Mechanical Engineering from Visveshwaraya Technological University in 2015. Presently working as automation Engineer at Indo-MIM Pvt. Ltd., Hoskote-562114.